

## RESEARCH ARTICLE

# Pulses within pulses: Concentration-discharge relationships across temporal scales in a snowmelt-dominated Rocky Mountain catchment

Robert Hensley<sup>1</sup>  | Joel Singley<sup>2,3</sup>  | Michael Gooseff<sup>4</sup> 

<sup>1</sup>National Ecological Observatory Network, Boulder, Colorado, USA

<sup>2</sup>Colorado School of Mines, Golden, Colorado, USA

<sup>3</sup>Department of Biology, Marine Biology, and Environmental Science, Roger Williams University, Bristol, Rhode Island, USA

<sup>4</sup>Institute of Arctic and Alpine Research, University of Colorado, Boulder, Colorado, USA

## Correspondence

Robert Hensley, National Ecological Observatory Network, Battelle, Boulder, CO, USA.

Email: [hensley@battelleecology.org](mailto:hensley@battelleecology.org)

## Funding information

United States National Science Foundation, Grant/Award Number: 1724433

## Abstract

Concentration-discharge (C-Q) relationships can provide insight into how catchments store and transport solutes, but analysis is often limited to long-term behaviour assessed from infrequent grab samples. Increasing availability of high-frequency sensor data has shown that C-Q relationships can vary substantially across temporal scales, and in response to different hydrologic drivers. Here, we present 4 years of dissolved organic carbon (DOC) and nitrate-nitrogen (NO<sub>3</sub>-N) sensor data from a snowmelt-dominated catchment in the Rocky Mountains of Colorado. We assessed both the direction (enrichment vs. dilution) and hysteresis in C-Q relationships across a range of time scales, from interannual to sub-daily. Both solutes exhibited a seasonal flushing response, with concentrations initially increasing as solute stores are mobilized by the melt pulse, but then declining as these stores are depleted. The high-frequency data revealed that the seasonal melt pulse was composed of numerous individual daily melt pulses. The solute response to daily melt pulses was relatively chemostatic, suggesting mobilization and depletion to be progressive rather than episodic processes. In contrast, rainfall-induced pulses produced short-lived but substantial enrichment responses, suggesting they may activate alternative solute sources or transport pathways. Finally, we observed low-level diel variation during summer baseflow following the melt pulse, likely driven by effects of daily evapotranspiration cycles. Additional contributions from in-stream metabolic cycles, independent from but covarying with diel streamflow cycles, could not be ruled out. The results clearly demonstrate that solute responses to daily cycles and individual events may differ significantly from the longer-term seasonal behaviour they combine to generate.

## KEYWORDS

concentration-discharge, DOC, high-frequency sensors, NEON, nitrate, snowmelt

## 1 | INTRODUCTION

Concentration-discharge (C-Q) relationships can provide valuable insights into how catchments store and transport solutes (Basu et al., 2011; Godsey et al., 2009; Godsey et al., 2019; Marinos

et al., 2020; Moatar et al., 2017; Musolff et al., 2017; Thompson et al., 2011). A negative C-Q relationship is indicative of a dilution response and often associated with source limitation, while a positive relationship is indicative of an enrichment response and often associated with transport limitation. C-Q responses are often hysteretic

(Lloyd et al., 2016; Musloff et al., 2021; Vaughan et al., 2017), with dissimilar C for the same Q during the rising versus falling limb of the hydrograph. This hysteresis can be useful in identifying the relative contributions of variable water sources (Bowes et al., 2005; Evans & Davies, 1998; House & Warwick, 1998). While long-term monitoring using grab sampling has proven incredibly useful in characterizing average catchment behaviour, low-temporal resolution datasets often cannot resolve the individual events that aggregate to compose the long-term trends (Knapp et al., 2020; Musloff et al., 2021).

Field deployable water chemistry sensors have revolutionized the frequency at which measurements can be recorded (Burns et al., 2019; Kirchner et al., 2004; Pellerin et al., 2016; Rode, Wade, et al., 2016), allowing characterization of processes varying over short time scales (Heffernan & Cohen, 2010; Pellerin et al., 2012). A key finding of recent sensor-based studies has been that just as the primary underlying hydrologic processes can vary from event to event and across temporal scales, so too can the C-Q responses (Duncan et al., 2017; Knapp et al., 2020; Koenig et al., 2017; Minaudo et al., 2019; Musloff et al., 2021; Rose et al., 2018; Werner et al., 2019; Wollheim et al., 2017). The direction and magnitude of hysteresis can similarly vary (Bieroza & Heathwaite, 2015; Blaen et al., 2017; Butturini et al., 2008; Fovet et al., 2018; Knapp et al., 2020; Lloyd et al., 2016; Musloff et al., 2021; Vaughan et al., 2017). Without high-frequency data, it might be incorrectly inferred that solute responses to changing Q at event scales might be identical to those observed over longer temporal scales.

Here we present high-frequency sensor measurements from a snowmelt dominated catchment, examining how C-Q dynamics vary across a range of temporal scales (interannual to sub-daily), and the implications for the underlying hydrological processes. In the western United States, around 75% of streamflow originates from seasonal snowmelt (Hamlet et al., 2007; Li et al., 2017). All catchments act as filters, damping variation in precipitation and solute inputs and generating blended outputs (Godsey et al., 2010; Kirchner et al., 2000; Thompson & Katul, 2012). Snowmelt dominated catchments are an extreme example where nearly all accumulated winter inputs are stored as snowpack and then released as a spring–summer melt pulse (Boyer et al., 1997; Creed & Band, 1998; Hornberger et al., 1994). These seasonal pulses represent the dominant hydrologic forcing over interannual time scales. However, closer inspection often reveals they are not singular pulses, but composed of numerous individual pulses (Kirchner et al., 2020; Krogh et al., 2021; Pellerin et al., 2012). These ‘pulses within the pulse’ originate from a combination of diel variation in rates of snowmelt (i.e., greater daytime melting) and also rain events which contribute additional water.

Using multiple years of sensor data, we examine the response of two reactive solutes, dissolved organic carbon (DOC) and nitrate-nitrogen ( $\text{NO}_3\text{-N}$ ), and a predominantly conservative tracer, specific conductance (SpC), to Q variation over a range of temporal scales. While the DOC and  $\text{NO}_3\text{-N}$  dynamics of snowmelt pulses have been extensively characterized at seasonal timescales using grab sampling (Boyer et al., 1997; Brooks et al., 1999; Hood, McKnight, et al., 2003; Hornberger et al., 1994), at higher frequencies they are critically

understudied (Pellerin et al., 2012). We demonstrate how the C-Q relationships and hysteresis patterns of individual daily melt and rain pulses, as well as diel baseflow variation driven by evapotranspiration (ET) are quantitatively distinct, both from each other, and from the patterns these events combine to generate over seasonal time scales.

## 2 | METHODS

### 2.1 | Site description

Como Creek (Figure 1) is located in the Niwot Ridge Long Term Ecological Research (LTER) site in Colorado, United States ( $40.035^\circ\text{N}$ ,  $105.545^\circ\text{W}$ ). It has an area of approximately  $5\text{ km}^2$ , with elevations ranging from 3000–3600 m above sea level. This makes it one of the highest catchments instrumented with in-situ water quality sensors anywhere in the world. Being located in an LTER, the carbon and nitrogen dynamics of Como Creek and the surrounding watersheds have been extensively studied (e.g., Brooks et al., 1996; Brooks et al., 1999; Brooks & Williams, 1999; Campbell et al., 1995; Campbell et al., 2000; Hood, McKnight, et al., 2003; Hood, Williams, et al., 2003; Williams et al., 1996; Williams et al., 2009). However, to our knowledge all previous studies have relied on grab sampling, and this will be the first study to use high-frequency sensors capable of resolving sub-daily variation in stream water chemistry.

The average annual precipitation is 730 mm, with roughly two thirds as snowfall (snowfall is reported as snow-water equivalent; SWE). Winters are long and cold, and summers are short and cool; mean air temperatures for January are  $-12^\circ\text{C}$ , and mean temperatures for July are  $12^\circ\text{C}$ . Typically, the stream is completely snow

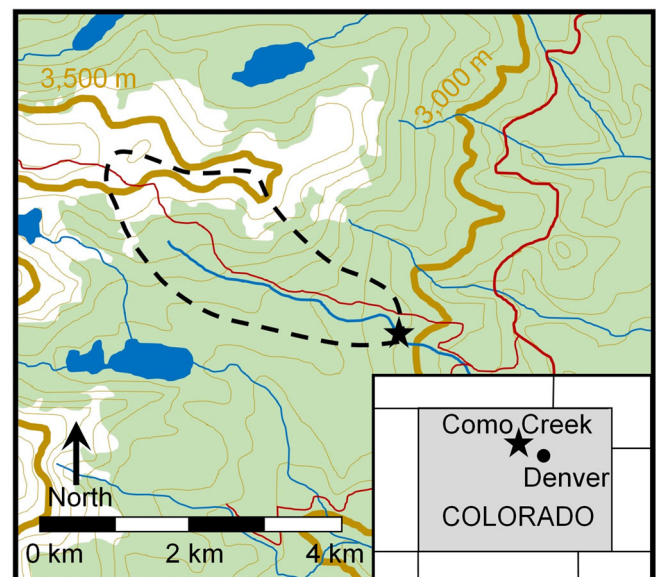


**FIGURE 1** Como Creek, Colorado. The inset shows the location within the state of Colorado. The star indicates the sampling location, dashed line is the approximate watershed boundary and green shows the approximate tree line

covered from late October until late May. The insulating effect of the overlying snow results in the stream water usually remaining just above freezing in the deeper pools, although winter Q is extremely small (within the rating curve uncertainty of being zero). The majority of the watershed is forested, consisting of Engelmann spruce (*Picea engelmannii*), subalpine fir (*Abies lasiocarpa*), limber pine (*Pinus flexilis*), lodgepole pine (*Pinus contorta* var. *latifolia*) and quaking aspen (*Populus tremuloides*). Approximately 15% of the watershed is above treeline, consisting of alpine tundra and scree slopes.

## 2.2 | Data provenance

We obtained 4 years (Oct 2017–Sep 2021) of high frequency data from the National Ecological Observatory Network (NEON). NEON (<https://neonscience.org>) is a National Science Foundation-funded network of monitoring sites throughout the United States providing long-term, open-access ecological data (Goodman et al., 2015). Since 2017, NEON maintained a monitoring reach along Como Creek, instrumented with a standardized suite of automated sensors (Hensley et al., 2021). Stream stage was recorded using Level Troll 500 vented pressure transducers (In-situ; Fort Collins CO). Manual Q measurements (26 per year) collected using an acoustic doppler velocimeter were used to develop rating curves for each water year (defined as 1 Oct through 30 Sep) and estimate continuous Q. Water quality measurements, including SpC and fluorescent dissolved organic matter (fDOM) were measured at one-minute intervals using an EXO2 multiparameter sonde (YSI; Yellow Springs OH). Stream NO<sub>3</sub>-N was measured using a submersible ultraviolet nitrate analyser (SeaBird Scientific, Bellevue WA) configured to take a 20-measurement burst at 15-min intervals. The first 10 bursts of each measurement were discarded to allow the SUNA lamp sufficient time to warm up; the remaining 10 measurements were averaged. The sensors remained installed throughout the winter, measuring concentrations in the liquid water under the ice and snow cover. Both the EXO2 and SUNA were equipped with automated wipers to prevent biofouling. They were also manually cleaned bi-weekly, and calibrated monthly.

We used the neonUtilities R package (Lunch et al., 2021), to download the following publicly available NEON datasets: continuous discharge (NEON, 2021a), water quality (NEON, 2021b), nitrate in surface water (NEON, 2021c), and chemical properties of surface water (NEON, 2021d). Quality flagged measurements were excluded from our analysis; this constituted a relatively small fraction of the total data (~5%) and the majority of these were periods in winter when the sensors temporarily became frozen in ice and were no longer measuring concentrations in the liquid water. Because these periods occurred when the stream was not flowing, there was little, if any, C-Q variation to observe. In a few instances, NEON maintenance and calibration records were used to correct for drift or calibration offsets in the data. Datasets published at higher frequencies (e.g., water quality) were averaged to 15-min intervals to match nitrate in surface water, which had the lowest temporal resolution. Short gaps of less than 6 h were filled using the na.spline function in the zoo R package (Zeileis et al., 2022). A linear regression between

bi-weekly manual DOC measurements and corresponding sensor fDOM measurements was used to estimate continuous DOC from the fDOM time-series (Supporting Figure S1). The R code used to download and process the NEON data, and perform subsequent analyses, is publicly available in a Zenodo repo (Hensley, 2022).

The NEON precipitation gage is located next to the NEON eddy flux tower, high on Niwot ridge, at an elevation (3500 m) much higher than most of the catchment. Therefore, daily precipitation and snow-pack data were obtained from the National Water and Climate Center Snow Telemetry (SNOTEL; <https://www.wcc.nrcs.usda.gov/snow/>) Niwot station (ID 663), which is located near the centre of the Como Creek catchment (3040 m) and likely more representative of the catchment.

## 2.3 | Data analysis

We quantified the solute response to the changing Q in several ways. First, we determined whether concentration versus discharge (C-Q) exhibited an enrichment, dilution, or chemostatic response. These relationships typically take the form of a power-law relationship ( $C = aQ^b$ ). A positive exponent  $b$  indicates enrichment, a near-zero ( $|b| < 0.2$ ) exponent indicates relative chemostasis, and a negative exponent indicates dilution (Basu et al., 2011; Godsey et al., 2009; Thompson et al., 2011).

We first fit the entire dataset to determine the C-Q response over interannual time scales. We then identified individual pulses within the dataset using the findpeaks function in the pracma R package (Borchers, 2022). Using the SNOTEL precipitation data, we determined which of these pulses were associated with rain events of at least 5 mm ( $>2\times$  the gage resolution) versus those primarily resulting from either daily melt cycles during the melt pulse, or summer base-flow. We fit the C-Q responses of these individual pulses to determine whether they behaved differently from each other, and from the interannual response.

Second, we quantified any hysteresis in the C-Q responses using a normalized hysteresis index (Lloyd et al., 2016; Musoff et al., 2021; Vaughan et al., 2017). For each event, discharge at each time step ( $\bar{Q}_t$ ) was first normalized relative to the minimum ( $Q_{min}$ ) and maximum ( $Q_{max}$ ).

$$\bar{Q}_t = \frac{Q_t - Q_{min}}{Q_{max} - Q_{min}}. \quad (1)$$

Concentration was then normalized in the same fashion.

$$\bar{C}_t = \frac{C_t - C_{min}}{C_{max} - C_{min}}. \quad (2)$$

This normalization creates a standardized scale allowing comparison between events of different magnitude. The hysteresis index (HI) is calculated from the difference in normalized concentration in rising limb of the event ( $\bar{C}_{RL}$ ) and the falling limb ( $\bar{C}_{FL}$ ).

$$HI = \overline{C_{RL}} - \overline{C_{FL}}. \quad (3)$$

Hysteresis loops can often take complex forms (e.g., figure-eights), so the *HI* should be evaluated at multiple *Q* values (Lloyd et al., 2016). For each event we evaluated *HI* along each 10% increment of  $\overline{Q}_t$  and then calculated an average *HI* for the entire event. The value of *HI* ranges from  $-1$  to  $1$ , with the absolute value indicating the magnitude of hysteresis, and the sign indicating the direction; positive = clockwise and negative = counter clockwise. Clockwise hysteresis suggests relative enrichment of earlier arriving water, while counter clockwise hysteresis suggests relative enrichment of later arriving water (Bowes et al., 2005; Evans & Davies, 1998; House & Warwick, 1998). For each solute, we used Student's *t*-tests to determine whether the variables characterizing the C-Q response (*b* and *HI*) were statically different for daily melt pulses versus rain pulses.

Finally, to quantifiably compare seasonal variability in the timing and magnitude of daily pulses, we fit a simple model (Kurz et al., 2013) to each day of data starting and ending at midnight. The model is based on a sine function with 24-h periodicity and three parameters: a mean value (*M*), an amplitude (*A*), and a phase (*P*).

$$C_t = M + A(\cos(t - P)2\pi). \quad (4)$$

The model was fit to the observed *Q* and solute data using non-linear least squares regression in R. For comparison, a single parameter model with no diel variation based on just the value *M* was also fit to the data. The F-statistic comparing the diel versus null models was calculated using the root sum of squares (RSS) and degrees of freedom (*df*). Whether a date window exhibited statistically significant diel variation was assessed using the F-statistic and resulting *p*-values.

$$F_{stat} = \frac{(RSS_{null} - RSS_{diel}) / (df_1 - df_2)}{RSS_{diel} / df_{diel}}. \quad (5)$$

Results from such analyses can be visualized using a polar plot with points representing the fitted model parameters for each day. Like a clock face, the angle signifies time of day of the peak, and the distance from the origin signifying the amplitude. These results should generally compliment the C-Q results. For example, alignment of solute and *Q* peak times would indicate a positive correlation corresponding to an enrichment response, while peak times perfectly out of phase would indicate a negative correlation corresponding to a dilution response. Likewise, the larger the amplitude of the solute peak relative to the amplitude of the *Q* peak, the greater the magnitude of the response. By also having the time of day, we can better characterize potential underlying mechanisms driving the variation.

### 3 | RESULTS

The annual snowmelt pulse typically began in early May, peaked in June, and had subsided by late July (Figure 2). The fitted C-Q relationships indicated that over interannual time scales DOC exhibited an

enrichment response (Figure 2d) while SpC exhibited a dilution response (Figure 2f). For NO<sub>3</sub>-N the exponent (*b*) was not statistically different from zero, indicating relative chemostasis (Figure 2e). Peak annual concentrations of both DOC and NO<sub>3</sub>-N preceded the melt pulse (Figure 2a,b), producing clockwise hysteresis over annual time scales (Figure 2d,e).

There was considerable intra-annual variation in the timing and magnitude of the seasonal melt pulse across the 4 years of NEON data. For example, the centroid of the pulse in 2019 was over 3 weeks later than in 2018, and total *Q* for 2019 was also over 60% higher than 2018 (Supporting Table 1). Historical LTER records from Como Creek (Williams et al., 2021) showed even greater intra-annual variation, with the date of the centroid varying by over a month, and the highest annual WY over three times higher than the lowest. The timing and magnitude of the seasonal melt pulse appeared correlated with the maximum depth of the snowpack, but also with how late the snowpack persisted into the spring. For example, while 2020 saw snowpack depth reach near-record levels in late April, it began to rapidly ablate and was gone by mid-May. In contrast, 2021 saw a 25% lower maximum depth, but it ultimately persisted into June and resulted in a later and larger melt pulse. While the focus of this paper is primarily on drivers of high-frequency variation, this intra-annual variation warrants mentioning given projections of reduced snowpack and an earlier snowmelt in coming decades (Clow, 2010; Dudley et al., 2017; Fritze et al., 2011; Marshall et al., 2019), and highlights the value of long-term, lower-frequency sampling (Burt et al., 2010).

The high-frequency data revealed that the melt pulse was not a singular pulse but composed of a multitude of individual daily melt pulses (Figures 3 and 4). These daily melt pulses were largest during the peak of snowmelt, with daily maxima regularly 25% greater than minima for the same day. Daily melt pulses typically peaked in the evening (Figure 5a), consistent with higher daytime rates of snowmelt. As the melt pulse receded, the amplitude began to decline and the peak time shifted later in time, consistent with ablation of the snowpack and a retreat to higher elevations, further from the catchment outlet where *Q* is being measured (Lundquist & Cayan, 2002). These large daily melt pulses did not appear to strongly impact the solute chemistry (Figure 3 and 4). For DOC, a *t*-test (Table 1) indicated that the mean of fitted C-Q exponents across these daily melt pulses was not statistically different from zero (Figure 6a), with few individual events where  $|b| > 0.2$  (Supporting Table 2). For DOC, *HI* values tended to be negative (Figure 6d), suggesting higher concentration on the falling limb of daily pulses. NO<sub>3</sub>-N exhibited a mean exponent (0.05) across daily pulses which was statistically non-zero (Figure 6b), but was also the solute with the most individual events which had non-significant exponents (Supporting Table 2). For NO<sub>3</sub>-N, *HI* values tended to be positive (Figure 6e), suggesting higher concentration on the rising limb of daily pulses. The mean exponent for SpC across daily melt pulses was also not significantly different from zero (Figure 6c), with very few individual events where  $|b| > 0.2$ .

Ultimately, as the seasonal melt pulse subsided and the stream moved into summer baseflow, the timing of daily *Q* variation settled onto early morning peaks (Figure 5a), consistent with ET becoming

**FIGURE 2** Time series of DOC (a), NO<sub>3</sub>-N (b) and SpC (c) from 1 Oct 2017 to 1 Oct 2021. Corresponding C-Q plots (d–f respectively) showed that over interannual time scales, DOC exhibited an enrichment response, NO<sub>3</sub>-N exhibited a chemostatic response (non-significant correlation) and SpC exhibited a dilution response. Seasonal DOC and NO<sub>3</sub>-N peaks preceded the melt pulse, resulting in clockwise hysteresis over interannual time scales. DOC, dissolved organic carbon

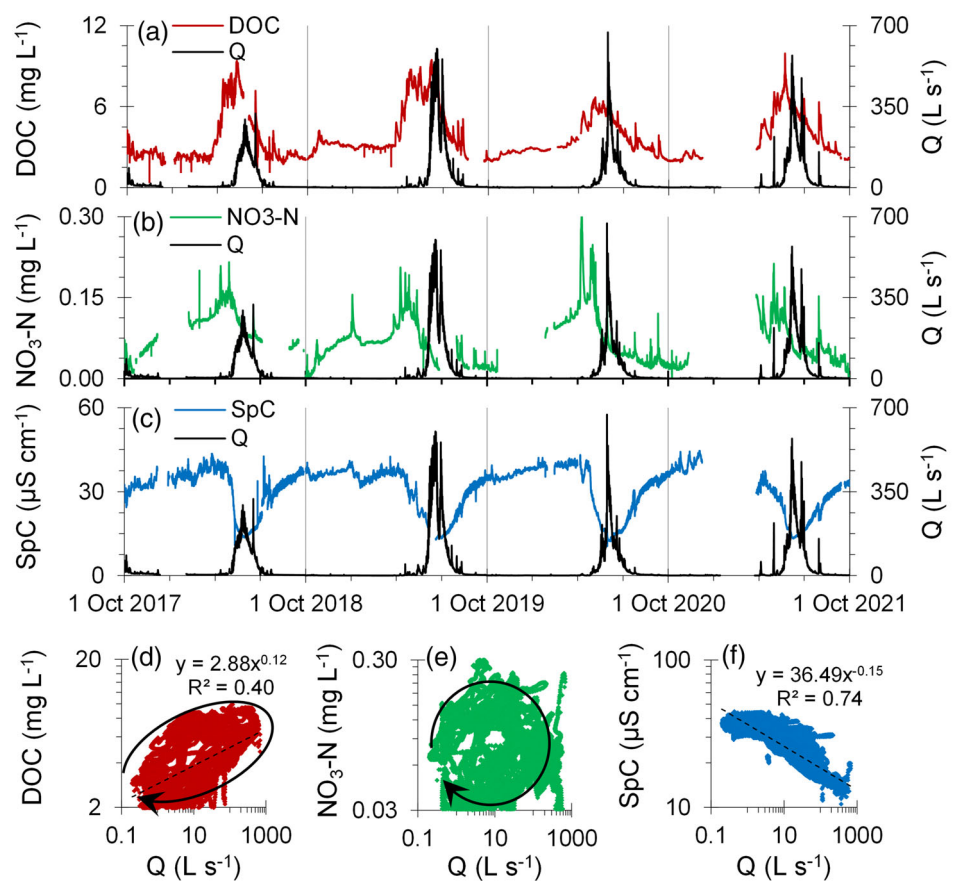


**TABLE 1** Summary of single-sample t-tests for C-Q exponent  $b$  across daily melt pulses and rain pulses

Parameter	t-stat	Df	Mean	Lower-95% CI	Upper-95% CI	p-value	
Melt pulses	$b_{\text{DOC}}$	0.69	69	0.01	-0.01	0.03	0.48
	$b_{\text{NO}_3\text{-N}}$	3.89	76	0.05	0.03	0.08	<0.01
	$b_{\text{SpC}}$	-1.41	58	-0.02	-0.04	0.01	0.16
Rain pulses	$b_{\text{DOC}}$	8.86	23	0.18	0.14	0.22	<0.01
	$b_{\text{NO}_3\text{-N}}$	7.56	19	0.42	0.31	0.54	<0.01
	$b_{\text{SpC}}$	-0.23	22	-0.00	-0.03	0.02	0.82

the dominant control on diel Q variation (Caine, 1992; Kirchner et al., 2020; Lundquist & Cayan, 2002). While orders of magnitude smaller in an absolute sense than the daily pulses seen during snowmelt, these daily interruptions of streamflow, or “non-pulses” are still quite large in a relative sense, with daily maxima regularly >50% greater than daily minima. Diel variation in water delivery due to ET is also capable of impacting solute chemistry (Hensley et al., 2017; Nimick et al., 2011). While diel variation in DOC, and NO<sub>3</sub>-N especially, were often close to the resolution of the sensors at baseflow, they did exhibit a fairly consistent amplitude and timing (Figure 5b–c). The amplitude of diel SpC variation actually appeared to increase from the melt pulse to baseflow (Figure 5d), despite order of magnitude decreases in the amplitude of daily Q variation. If SpC is trusted as a conservative tracer, this potentially suggests wider relative swings in source water throughout the day during baseflow relative to during the melt pulse. These small daily baseflow variations (Figure 7a–c)

created their own C-Q dynamics and hysteresis loops, counterclockwise for DOC, and clockwise for NO<sub>3</sub>-N and SpC (Figure 7d–i).

In contrast to daily melt pulses, both DOC and NO<sub>3</sub>-N consistently showed enrichment responses to pulses generated by rain events (Figures 3 and 4). The fitted C-Q exponents across rain pulses were universally positive (Supporting Table 3), with means across all events of 0.18 for DOC and 0.42 for NO<sub>3</sub>-N (Figure 6a,b). Student’s t-tests indicate that fitted exponents for rain pulses were statistically greater than for daily melt pulses. Values of the  $HI$  during rain pulses were universally negative for DOC (Figure 6d), and for most NO<sub>3</sub>-N (Figure 6e). This counterclockwise hysteresis (Figure 3e–h and 4e–j) indicates DOC and NO<sub>3</sub>-N concentrations tend to be higher on the falling limb of rain pulses. SpC in contrast did not exhibit a strong response to rain pulses, with a mean across events that was not statistically different from zero (Figure 6c). The only two rain pulses producing SpC exponents with a  $|b| > 0.15$  were both rain on snow events.

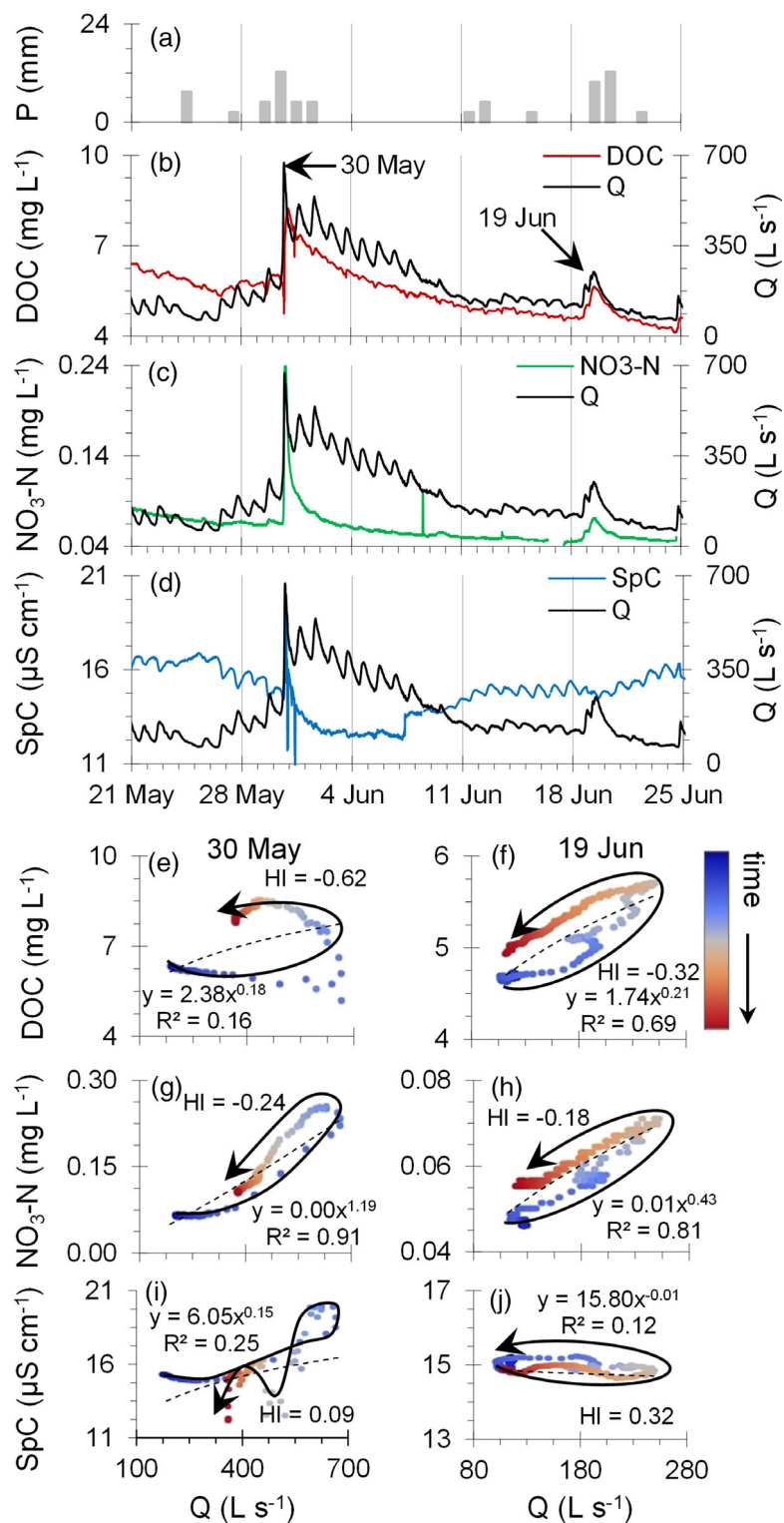


**FIGURE 3** Time series of precipitation (a), DOC (b), NO<sub>3</sub>-N (c) and SpC (d) from 21 May to 25 Jun 2020. The seasonal melt pulse can be seen to the left. C-Q plots of rain pulses illustrate DOC (e-f) and NO<sub>3</sub>-N (g-h) were enriched by rain pulses, with counter-clockwise hysteresis. SpC was enriched by a rain on snow event on 30 May (i) but showed a relatively chemostatic response to later rain pulses (j). Note that large daily melt pulses not associated with rain did not produce the same responses. DOC, dissolved organic carbon

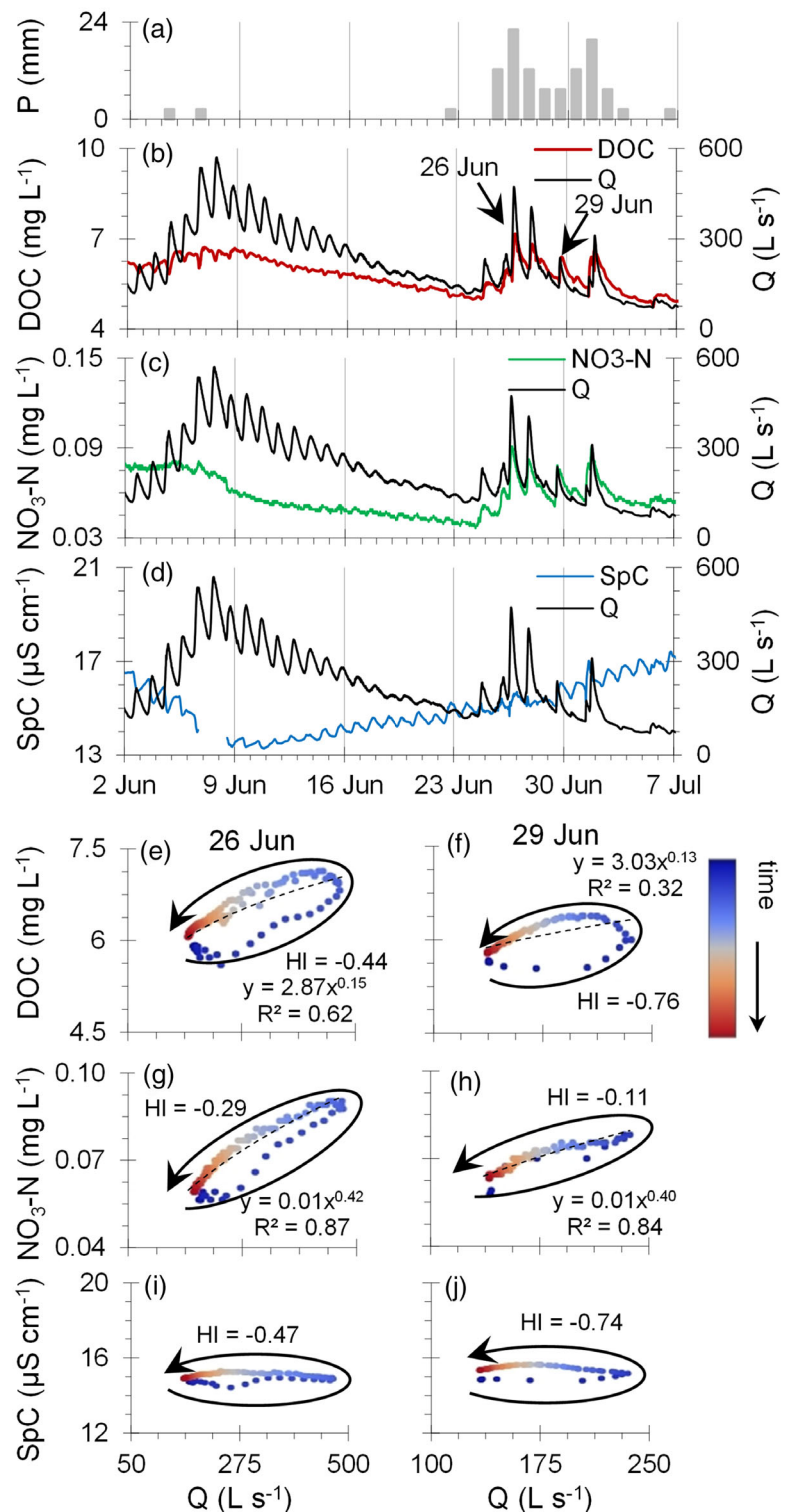
## 4 | DISCUSSION

### 4.1 | Seasonal and daily melt pulses

Seasonally, peak DOC and NO<sub>3</sub>-N concentrations both preceded the melt pulse, resulting in clockwise C-Q hysteresis over seasonal time scales (Figure 2). This suggests that stores of solutes built up over

periods of low flow are flushed out by the seasonal melt pulse. However, there are several key differences between DOC and NO<sub>3</sub>-N, which were also not perfectly in phase with each other either. In the case of DOC, concentrations begin increasing in the beginning of spring, around the time the stream is just starting to flow. DOC concentrations peak as the melt pulse begins in earnest, at which point they then begin to decline. The seasonal offset between DOC and Q

**FIGURE 4** Time series of precipitation (a), DOC (b),  $\text{NO}_3\text{-N}$  (c) and SpC (d) from 2 Jun to 7 Jul 2021. The seasonal melt pulse can be seen in the centre. C-Q plots of rain pulses illustrate DOC (e–f) and  $\text{NO}_3\text{-N}$  (g–h) were enriched by rain pulses, with counter-clockwise hysteresis. SpC (i–j) showed a relatively chemostatic response to rain pulses. Note that large daily melt pulses not associated with rain did not produce the same responses. DOC, dissolved organic carbon



signals is only about a month, resulting in the modest positive correlation over interannual time scales (Figure 2e). In contrast, seasonal increases in  $\text{NO}_3\text{-N}$  begin much earlier than DOC. In fact, they seem to begin almost as soon the stream freezes over in late autumn.  $\text{NO}_3\text{-N}$  concentrations also begin declining much earlier, at a time well before DOC concentrations have reached their peak. There is much less of an interannual correlation between  $\text{NO}_3\text{-N}$  and Q (Figure 2f) because the seasonal offset

between the  $\text{NO}_3\text{-N}$  and Q signals is closer to 2 months. These differences in timing reflect the contrasting mechanisms responsible for solute generation over seasonal time scales.

Previous studies in Como Creek (Hood, McKnight, et al., 2003) and other nearby catchments in Colorado (Boyer et al., 1997; Brooks et al., 1999; Hornberger et al., 1994) have interpreted the seasonal DOC signal as the flushing of a reservoir which has built up within the

catchment subsurface during winter periods of little or no flow. Concentrations of DOC within the snowpack are lower than in stream or sediment porewater, averaging  $1\text{--}1.5\text{ mg L}^{-1}$  (Williams et al., 2009). Flushing of stored DOC causes concentrations to initially rise as the stream begins flowing but are subsequently diluted by large volumes of newer melt water. In contrast, concentrations of inorganic N, including  $\text{NO}_3\text{-N}$ , were found to be much higher in the snowpack than in sediment porewater, where organic N was the dominant form of N (Hood, Williams, et al., 2003; Williams et al., 2009). Concentrations of  $\text{NO}_3\text{-N}$  within the snowpack increase over the winter (Brooks & Williams, 1999) often reaching values of  $0.15\text{ mg L}^{-1}$  (Williams et al., 2009), similar to what was observed in the stream during this study. While frozen over and mostly stagnant, stream water may begin to reflect  $\text{NO}_3\text{-N}$  concentrations in the overlying snowpack (Campbell et al., 1995). Notably, slight melting of overlying snow

during April freeze–thaw cycles, can transfer  $\text{NO}_3\text{-N}$  directly from the snowpack to the stream (Williams & Melack, 1991). While often almost imperceptible on the Q hydrograph, the spikes produced by these events typically produce the highest annual  $\text{NO}_3\text{-N}$  concentrations. Once the stream begins flowing,  $\text{NO}_3\text{-N}$  is flushed by water that has infiltrated through the subsurface and undergone transformation from inorganic to organic N.

It is worth noting that the apparent seasonal depletion of solute stores within the catchment may not be entirely the result of hydrologic export. As temperatures warm, increased reactivity (e.g., respiration of DOC and assimilation or denitrification of  $\text{NO}_3\text{-N}$ ) could also be contributing to the observed signal. NEON performs low-frequency sampling of groundwater concentrations (twice per year, preceding and following the melt pulse). Single-tailed paired t-tests of individual wells within years (Supporting Table 4) indicate a statistically significant decrease in groundwater DOC concentrations following the melt pulse ( $p = 0.02$ ). While there was a simultaneous increase in specific ultraviolet absorbance at 254 nm ( $\text{SUVA}_{254}$ ), it was non-significant ( $p = 0.08$ ). This leaves it unclear whether any preferential biogeochemical depletion of less recalcitrant DOC is occurring, or whether DOC is simply being flushed en masse.

The solute responses to daily melt pulses within the larger seasonal pulse were relatively modest (Figure 6). The relative chemostasis suggests that daily melt pulses are composed of variable amounts of water with relatively similar chemistry. The flushing responses observed at seasonal scales do not occur in response to daily melt pulses or are at least substantially muted. This suggests a large reservoir of solutes, and that depletion and regeneration are slow, progressive processes occurring over times scales of weeks and months rather than an episodic process occurring over time scales of hours.

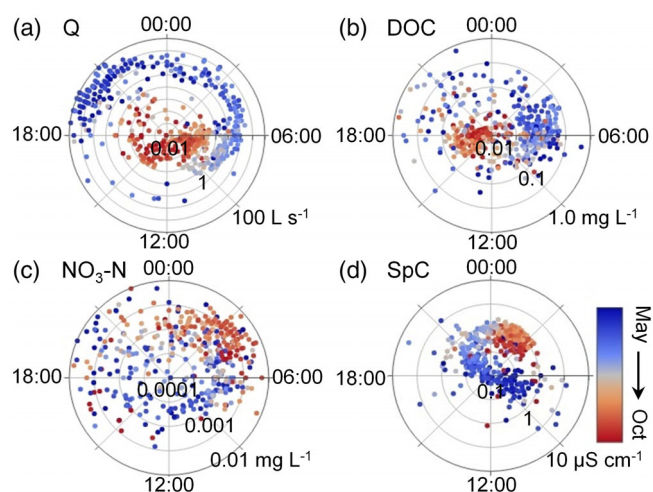


**FIGURE 5** Diel timing and amplitude of Q (a), DOC (b),  $\text{NO}_3\text{-N}$  (c) and SpC (d). Radial position indicates time of daily maxima and distance from origin indicates amplitude. Colour scales go from the beginning of the melt pulse in early May (blue) to the end of summer baseflow in late October (red). DOC, dissolved organic carbon

#### 4.2 | Diel variation – Hydrologic or biologic?

We observed diel C-Q patterns during summer baseflow (Figure 7), and these often varied from those observed over interannual time

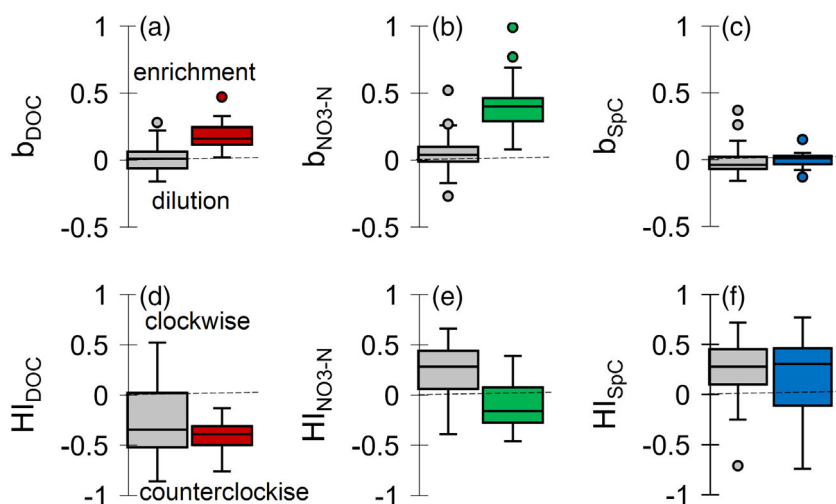


**FIGURE 6** Distribution of C-Q exponents (a–c) and HI (d–f) for DOC (left),  $\text{NO}_3\text{-N}$  (middle) and SpC (right). Plots show range, inner quartiles and median, with outliers denoted by circles. Note the often-differing responses to daily melt pulses (grey) and rain pulses (coloured). DOC, dissolved organic carbon

scales. For example, while DOC and Q still showed a long-term positive correlation (simultaneously declining over the week of data shown in Figure 7a), on individual days they show a negative correlation (Figure 7d,e). However, from the data available to us, it was not entirely clear whether diel Q variation alone was responsible for diel solute variation, a potential case of correlation without causation.

The baseflow timing of daytime DOC maxima and NO<sub>3</sub>-N minima (Figure 7) was consistent with in-stream primary production and coupled autotrophic assimilation of N (Heffernan & Cohen, 2010; Oviedo-Vargas et al., 2022; Roberts & Mulholland, 2007; Rode, Angelstein, et al., 2016; Sullivan et al., 1998). However, most of Como Creek is narrow and heavily shaded throughout the year, limiting light availability for photosynthesis (Savoy & Harvey, 2021). Even with low, primary production, diel signals could still result from non-autotrophic in-stream processes such as denitrification, which would be stimulated by warmer daytime water temperatures (Rusjan & Mikoš, 2010).

Combined with the simultaneous diel variation in Q driven by ET, it is likely that the diel DOC and NO<sub>3</sub>-N signals are at least partially driven by diel variation in the water being delivered to the stream. This is further supported by the simultaneously large diel variation in SpC, though it is worth noting that SpC is not entirely conservative and diel SpC cycles can be generated by biogeochemical processing in highly productive streams (De Montety et al., 2011; Kurz et al., 2013).

Diel solute signals are often driven by a combination of hydrologic delivery and in-stream biogeochemical processes (Hensley et al., 2017; McKnight & Bencala, 1990; Mulholland & Hill, 1997; Nimick et al., 2011; Oviedo-Vargas et al., 2022), with the former often dominating during periods of high Q and the latter during periods of low flow (Hensley et al., 2019). Given the large volumes of water, short in-stream residence times and cold-water temperatures, we feel confident that variation in solute chemistry during the melt pulse is primarily driven by variation in delivery to the stream. However, this may not be the case at baseflow. Further work is needed to better constrain rates of in-stream biogeochemical processing in order to fully assess their impact on the observed C-Q dynamics at different timescales.

### 4.3 | Rain pulses

In contrast to daily melt pulses, rain pulses tended to strongly enrich DOC and NO<sub>3</sub>-N concentrations (Figure 6). This enrichment occurred continually throughout the year even during periods well after concentrations had otherwise shown signs of seasonal depletion. Even where rain pulses occurred over multiple successive days (e.g., Figure 4), concentrations continued to be enriched. It suggests that rain pulses are somehow able to consistently mobilize additional sources, or short circuit retention along transport pathways. While this enrichment was clearly evident from the data, multiple combinations of physical processes are capable of generating similar responses (Butturini et al., 2008; Chanut et al., 2002; Musolff et al., 2017), making identification difficult. Below, we offer several possible explanations.

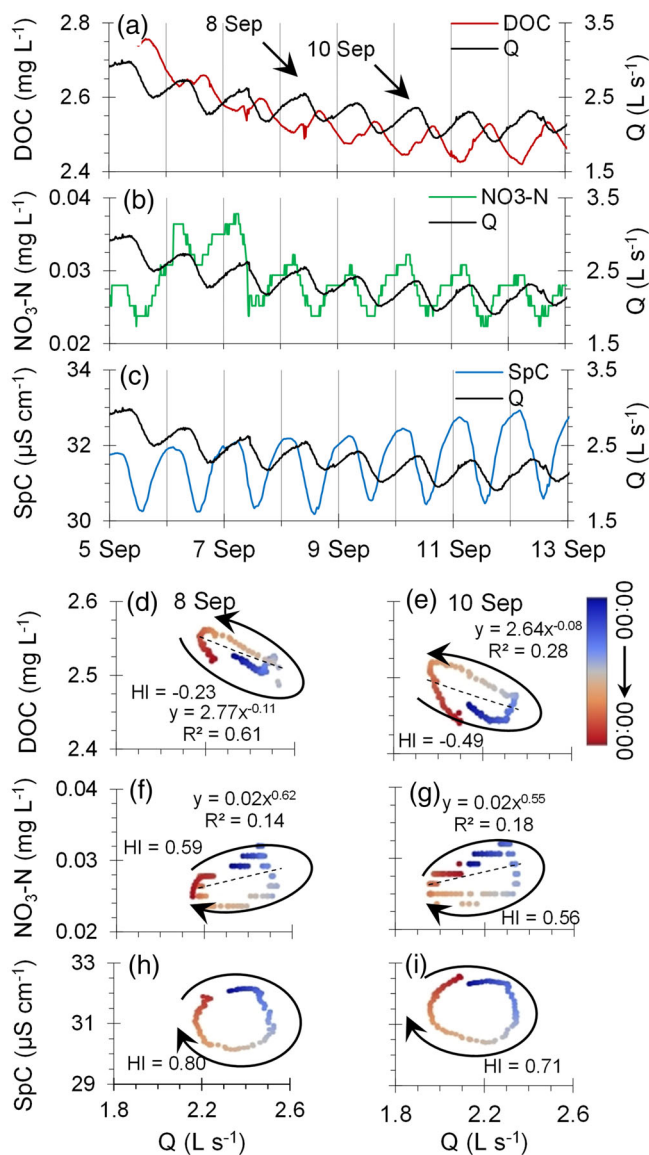


**FIGURE 7** Time series of DOC (a), NO<sub>3</sub>-N (b) and SpC (c) during baseflow period from 5 Sep to 13 Sep 2021. C-Q plots for select days showed that over daily time scales, DOC exhibited a dilution response with counter clockwise hysteresis (d–e), NO<sub>3</sub>-N exhibited an enrichment response with clockwise hysteresis (f–g) and SpC exhibited a chemostatic (non-significant) response with clockwise hysteresis. It is unclear if these correlations indicate causation, as diel solute signals could arise from biogeochemical as well as hydrological processes. DOC, dissolved organic carbon

Elution of solutes directly from the snowpack may explain what is happening in the rain on snow events, for example on 30 May 2020 (Figure 3). For NO<sub>3</sub>-N in particular, May and early June rain on snow events typically produced the largest enrichment responses, and unlike rain pulses later in the summer, they also appeared to produce a strong response in SpC (Supporting Table 3). While DOC is generally low in the snowpack, any infiltrating water from these early season rain events will also find more abundant stores of DOC to flush out of the subsurface. However, while permanent snowfields and glaciers

are present in adjacent catchments, there are none in Como Creek. Enrichment of DOC and  $\text{NO}_3\text{-N}$  by rain pulses continued to occur late into the summer when the snowpack was no longer present, indicating solute elution from the snowpack cannot be the only additional source being mobilized by rain events.

One possible way that rainfall may mobilize additional stores is by temporarily establish greater connectivity with the more distal portions of the catchment (Casson et al., 2014; Hood et al., 2006; Kiewiet et al., 2020). Past work in Como Creek and the surrounding catchments have indicated that while sediment porewater in the lower elevation, forested parts of the catchment are potentially N-limited and low in  $\text{NO}_3\text{-N}$  (Hood, Williams, et al., 2003; Williams et al., 2009), the talus slopes and tundra soils of the higher elevation parts of the catchment receive greater atmospheric deposition of  $\text{NO}_3\text{-N}$  (Williams et al., 1996) and are less productive (Campbell et al., 2000; Clow & Sueker, 2000), resulting in greater availability of  $\text{NO}_3\text{-N}$  (Sueker et al., 2001; Hood, Williams, et al., 2003). Increased connectivity with these more distal regions of the catchment and their greater stores of  $\text{NO}_3\text{-N}$  could explain the enrichment of  $\text{NO}_3\text{-N}$  following rain events. The counter clockwise hysteresis, indicating later arriving water to be more enriched relative earlier arriving water, is also consistent with the greater distance from these source areas to the sensor station at the catchment outlet. However, the same low productivity also results in these higher elevations having much lower DOC concentrations (Hood, McKnight, et al., 2003). It would therefore be expected that greater connectivity with these areas would tend to dilute DOC concentrations and produce clockwise hysteresis, yet this is not what was observed in the data. Surprisingly, the marked spatial differences in sediment water chemistry within the catchment do not appear to be reflected in the temporal response to rainfall, where both DOC and  $\text{NO}_3\text{-N}$  behaved very similar.

A second possible explanation is that faster velocities and activation of alternative flow paths resulting from rain pulses shunt the reactive capacity (Raymond et al., 2016). Based on the previous studies, shorter travel times would be expected to result in reduced uptake and conversion of  $\text{NO}_3\text{-N}$  to alternative forms or removal through denitrification. However, these same studies suggest that at least for snowmelt, DOC is gained rather than lost via transport through the catchment. It may be that rainfall-generated quickflow through the soil active zone, while faster, may still be able to pick up more DOC given the proximity to where organic carbon is being stored.

A third intriguing explanation is that solutes are being sourced from the rainfall itself. Notably, DOC concentrations in summer wet deposition at Niwot Ridge can regularly be up to four and occasionally even  $10 \text{ mg L}^{-1}$  (Mladenov et al., 2012), higher than stream water concentrations during much of the year. Concentrations of  $\text{NO}_3\text{-N}$  in summer wet deposition are similarly elevated (mean =  $0.4 \text{ mg L}^{-1}$ ; Mladenov et al., 2012). Additional studies (e.g., Oldani et al., 2017) confirm shifts in the predominant wind direction can result in higher concentrations of both DOC and  $\text{NO}_3\text{-N}$  in summer rainfall versus winter snowfall. This suggests the alternative “source” being mobilized may potentially be the rainwater itself. This is a surprising

possibility, and one we were not expecting. While these changes in chemistry of wet deposition have been well documented (Mladenov et al., 2012; Oldani et al., 2017), to our knowledge a resulting response in stream water chemistry to large rainfall events has not been reported in any previous studies of Como Creek or surrounding catchments of Niwot Ridge LTER, likely because they relied on grab sampling with insufficient temporal resolution to resolve it (e.g., Williams, 2021). Even this last explanation requires some reconciling, as the counter clockwise hysteresis direction is inconsistent with traditional conceptual models of enrichment by early arriving water in the form of direct rainfall inputs and surface runoff (Evans & Davies, 1998). One possibility is that Q during the rising limb of the rain pulse consists of a mixture of new runoff and much older, less enriched water being flushed out of the sediment porewater by infiltrating rainfall; peak event water fraction often lags peak Q (Litt et al., 2015; von Freyberg et al., 2017). In addition, the falling limb of rain pulses may also consist of more late arriving water from the higher elevations of the catchment which is above treeline (less interception) and less reactive. The stream channel distance from the sensor station to treeline is  $\sim 3.5 \text{ km}$  and the mean velocity is around  $\sim 0.3 \text{ m s}^{-1}$ , making the timing lag between peak Q and peak solute concentrations following rain events of  $\sim 3 \text{ h}$  at least consistent with these explanations.

While the data clearly show a DOC and  $\text{NO}_3\text{-N}$  enrichment response to rainfall events, the exact mechanisms require further investigation. Isotopic composition (von Freyberg et al., 2017) and specific ultraviolet absorbance (Hood et al., 2006; Saraceno et al., 2009) could be used to better characterize water age and solute sources. While NEON grab samples include these measurements, they were not collected at nearly the required temporal frequency to resolve individual rain events. From a spatial perspective, simultaneous collection of data at multiple locations throughout the catchment could prove equally informative in identifying solute sources. While these have also previously been collected and show the general longitudinal trends in stream and sediment water chemistry (Hood, Williams, et al., 2003), they are of insufficient temporal resolution to show the propagation of solute pulses through the catchment at the scale of individual rain events.

## 5 | CONCLUSIONS

Using high-frequency sensors, we demonstrated that seasonal snowmelt pulses in an alpine catchment are not singular events but composed of numerous individual ‘pulses within the pulse,’ resulting from daily melt cycles, rainfall and ET. The C-Q dynamics varied across temporal scales, and the response to individual events occurring over short time scales often did not align with the response these same events combine to generate over longer time scales. Seasonal melt pulses exhibited clockwise C-Q hysteresis, consistent with a flushing response; concentrations of DOC and  $\text{NO}_3\text{-N}$  initially increasing as stores became mobilized, but then decreasing as these stores were depleted. The daily melt pulses which made up the seasonal melt

pulse did not produce a similar response; they were largely chemostatic, suggesting depletion and regeneration to be cumulative rather than episodic processes. Rain pulses in contrast were able to consistently enrich solute concentrations, though uncertainty remains over the exact mechanisms.

While in-situ solute sensors are a power tool and a very much in vogue frontier in watershed science, it is important to remember they have limitations. Using a single time-series from the outlet to definitively identify spatially distributed processes occurring throughout the catchment can be tenuous at best, no matter how high-frequency the data may be. Multiple combinations of processes can generate similar C-Q responses, potentially resulting in specious inferences. Moreover, solute signals represent the convolution of multiple processes, both hydrological and biological, which cannot easily be deconvolved without additional information. This poses challenges, but also presents opportunities for new types of sensors, sampling design and analytical methods.

As the climate changes, a greater fraction of precipitation is projected to fall as rain rather than snow (Kampf & Lefsky, 2016) and mid-winter freeze/thaw cycles may become more common (Jennings & Molotch, 2020) at Como Creek. This is true of other snowmelt dominated catchments in the central Rocky Mountains in general (Fritze et al., 2011). This transition in export regime from a seasonal pulse to more episodic events distributed throughout the year will put a greater emphasis on using sensors to characterize the C-Q dynamics of these higher frequency events. Documenting these responses to changing climate, land use and other anthropogenic impacts is one of the explicit objectives of NEON over its 30 year life.

## ACKNOWLEDGEMENTS

NEON is a National Science Foundation funded project operated by Battelle Memorial Institute (Award 1724433). We thank H. Schartel, Z. Lafaver, R. Lehrter and the field staff of NEON Domain 10/13 for data collection and sensor maintenance.

## DATA AVAILABILITY STATEMENT

All data used in this manuscript is publicly available on the NEON data portal (<https://data.neonscience.org>). The R code used for analysis is publicly available in Zenodo (<https://doi.org/10.5281/zenodo.6600430>).

## ORCID

Robert Hensley  <https://orcid.org/0000-0001-8542-087X>

Joel Singley  <https://orcid.org/0000-0002-7906-8491>

Michael Gooseff  <https://orcid.org/0000-0003-4322-8315>

## REFERENCES

- Basu, N. B., Thompson, S. E., & Rao, P. S. C. (2011). Hydrologic and biogeochemical functioning of intensively managed catchments: A synthesis of top-down analyses. *Water Resources Research*, 47, W00J15. <https://doi.org/10.1029/2011wr010800>
- Bierozza, M. Z., & Heathwaite, A. L. (2015). Seasonal variation in phosphorus concentration-discharge hysteresis inferred from high-frequency in situ monitoring. *Journal of Hydrology*, 524, 333–347. <https://doi.org/10.1016/j.jhydrol.2015.02.036>
- Blaen, P. J., Khamis, K., Lloyd, C., Comer-Warner, S., Ciocca, F., Thomas, R. M., MacKenzie, A. R., & Krause, S. (2017). High-frequency monitoring of catchment nutrient exports reveals highly variable storm event responses and dynamic source zone activation. *Journal of Geophysical Research: Biogeosciences*, 122(9), 2265–2281. <https://doi.org/10.1002/2017JG003904>
- Borchers, H.W. (2022). Practical numerical math functions. R package version 2.3.8. <https://CRAN.R-projects.org/package=pracma>
- Bowes, M. J., House, W. A., Hodgkinson, R. A., & Leach, D. V. (2005). Phosphorus-discharge hysteresis during storm events along a river catchment: The river swale, UK. *Water research*, 39(5), 751–762. <https://doi.org/10.1016/j.watres.2004.11.027>
- Boyer, E. W., Hornberger, G. M., Bencala, K. E., & McKnight, D. M. (1997). Response characteristics of DOC flushing in an alpine catchment. *Hydrological Processes*, 11(12), 1635–1647.
- Brooks, P. D., McKnight, D. M., & Bencala, K. E. (1999). The relationship between soil heterotrophic activity, soil dissolved organic carbon (DOC) leachate, and catchment-scale DOC export in headwater catchments. *Water Resources Research*, 35(6), 1895–1902. <https://doi.org/10.1029/1998WR900125>
- Brooks, P. D., & Williams, M. W. (1999). Snowpack controls on nitrogen cycling and export in seasonally snow-covered catchments. *Hydrological Processes*, 13(14–15), 2177–2190.
- Brooks, P. D., Williams, M. W., & Schmidt, S. K. (1996). Microbial activity under alpine snowpacks, Niwot Ridge, Colorado. *Biogeochemistry*, 32(2), 93–113. <https://doi.org/10.1007/BF00000354>
- Burns, D. A., Pellerin, B. A., Miller, M. P., Capel, P. D., Tesoriero, A. J., & Duncan, J. M. (2019). Monitoring the riverine pulse: Applying high-frequency nitrate data to advance integrative understanding of biogeochemical and hydrological processes. *Wiley Interdisciplinary Reviews-Water*, 6(4), e1348. <https://doi.org/10.1002/wat2.1348>
- Burt, T. P., Howden, N. J. K., Worrall, F., & Whelan, M. J. (2010). Long-term monitoring of river water nitrate: How much data do we need? *Journal of Environmental Monitoring*, 12(1), 71–79. <https://doi.org/10.1039/B913003A>
- Butturini, A., Alvarez, M., Bernal, S., Vazquez, E., & Sabater, F. (2008). Diversity and temporal sequences of forms of DOC and NO<sub>3</sub>-discharge responses in an intermittent stream: Predictable or random succession? *Journal of geophysical research. Biogeosciences*, 113(G3). <https://doi.org/10.1029/2008JG000721>
- Caine, N. (1992). Modulation of the diurnal streamflow response by the seasonal snowcover of an alpine basin. *Journal of Hydrology*, 137(1–4), 245–260. [https://doi.org/10.1016/0022-1694\(92\)90059-5](https://doi.org/10.1016/0022-1694(92)90059-5)
- Campbell, D. H., Baron, J. S., Tonnessen, K. A., Brooks, P. D., & Schuster, P. F. (2000). Controls on nitrogen flux in alpine/subalpine watersheds of Colorado. *Water Resources Research*, 36(1), 37–47. <https://doi.org/10.1029/1999WR900283>
- Campbell, D. H., Clow, D. W., Ingersoll, G. P., Mast, M. A., Spahr, N. E., & Turk, J. T. (1995). Processes controlling the chemistry of two snowmelt-dominated streams in the Rocky Mountains. *Water Resources Research*, 31(11), 2811–2821. <https://doi.org/10.1029/95WR02037>
- Casson, N. J., Eimers, M. C., & Watmough, S. A. (2014). Sources of nitrate export during rain-on-snow events at forested catchments. *Biogeochemistry*, 120(1), 23–36. <https://doi.org/10.1007/s10533-013-9850-4>
- Chanat, J. G., Rice, K. C., & Hornberger, G. M. (2002). Consistency of patterns in concentration-discharge plots. *Water Resources Research*, 38(8), 22–21. <https://doi.org/10.1029/2001WR000971>
- Clow, D. W. (2010). Changes in the timing of snowmelt and streamflow in Colorado: A response to recent warming. *Journal of Climate*, 23(9), 2293–2306. <https://doi.org/10.1175/2009JCLI2951.1>

- Clow, D. W., & Sueker, J. K. (2000). Relations between basin characteristics and stream water chemistry in alpine/subalpine basins in Rocky Mountain National Park, Colorado. *Water Resources Research*, 36(1), 49–61. <https://doi.org/10.1029/1999WR900294>
- Creed, I. F., & Band, L. E. (1998). Export of nitrogen from catchments within a temperate forest: Evidence for a unifying mechanism regulated by variable source area dynamics. *Water Resources Research*, 34(11), 3105–3120. <https://doi.org/10.1029/98WR01924>
- De Montety, V., Martin, J. B., Cohen, M. J., Foster, C., & Kurz, M. J. (2011). Influence of diel biogeochemical cycles on carbonate equilibrium in a karst river. *Chemical Geology*, 283(1–2), 31–43. <https://doi.org/10.1016/j.chemgeo.2010.12.025>
- Dudley, R. W., Hodgkins, G. A., McHale, M. R., Kolian, M. J., & Renard, B. (2017). Trends in snowmelt-related streamflow timing in the conterminous United States. *Journal of Hydrology*, 547, 208–221. <https://doi.org/10.1016/j.jhydrol.2017.01.051>
- Duncan, J. M., Band, L. E., & Groffman, P. M. (2017). Variable nitrate concentration–discharge relationships in a forested watershed. *Hydrological Processes*, 31(9), 1817–1824. <https://doi.org/10.1002/hyp.11136>
- Evans, C., & Davies, T. D. (1998). Causes of concentration/discharge hysteresis and its potential as a tool for analysis of episode hydrochemistry. *Water Resources Research*, 34(1), 129–137. <https://doi.org/10.1029/97WR01881>
- Fovet, O., Humbert, G., Dupas, R., Gascuel-Oudou, C., Gruau, G., Jaffrezic, A., Thelusma, G., Faucheux, M., Gilliet, N., Hamon, Y., & Grimaldi, C. (2018). Seasonal variability of stream water quality response to storm events captured using high-frequency and multi-parameter data. *Journal of Hydrology*, 559, 282–293. <https://doi.org/10.1016/j.jhydrol.2018.02.040>
- Fritze, H., Stewart, I. T., & Pebesma, E. (2011). Shifts in western north American snowmelt runoff regimes for the recent warm decades. *Journal of Hydrometeorology*, 12(5), 989–1006. <https://doi.org/10.1175/2011JHM1360.1>
- Godsey, S. E., Aas, W., Clair, T. A., De Wit, H. A., Fernandez, I. J., Kahl, J. S., Malcolm, I. A., Neal, C., Neal, M., Nelson, S. J., Norton, S. A., Palucis, M. C., Skjelkvåle, B. L., Soulsby, C., Tetzlaff, D., & Kirchner, J. W. (2010). Generality of fractal 1/f scaling in catchment tracer time series, and its implications for catchment travel time distributions. *Hydrological Processes*, 24(12), 1660–1671. <https://doi.org/10.1002/hyp.7677>
- Godsey, S. E., Hartmann, J., & Kirchner, J. W. (2019). Catchment chemostasis revisited: Water quality responds differently to variations in weather and climate. *Hydrological Processes*, 33, 3056–3069. <https://doi.org/10.1002/hyp.13554>
- Godsey, S. E., Kirchner, J. W., & Clow, D. W. (2009). Concentration–discharge relationships reflect chemostatic characteristics of US catchments. *Hydrological Processes*, 23(13), 1844–1864. <https://doi.org/10.1002/Hyp.7315>
- Goodman, K. J., Parker, S. M., Edmonds, J. W., & Zeglin, L. H. (2015). Expanding the scale of aquatic sciences: The role of the National Ecological Observatory Network (NEON). *Freshwater Science*, 34(1), 377–385. <https://doi.org/10.1086/679459>
- Hamlet, A. F., Mote, P. W., Clark, M. P., & Lettenmaier, D. P. (2007). Twentieth-century trends in runoff, evapotranspiration, and soil moisture in the western United States. *Journal of Climate*, 20(8), 1468–1486. <https://doi.org/10.1175/JCLI4051.1>
- Heffernan, J. B., & Cohen, M. J. (2010). Direct and indirect coupling of primary production and diel nitrate dynamics in a subtropical spring-fed river. *Limnology and Oceanography*, 55(2), 677–688. <https://doi.org/10.4319/lo.2010.55.2.0677>
- Hensley, R. (2022). Como Creek Colorado C-Q data (version 1.0.0) [Data set]. Zenodo <https://doi.org/10.5281/zenodo.6600430>
- Hensley, R., Harrison, N., Goodman, K., Cawley, K., Litt, G., Nance, B., & Catolico, N. (2021). A comparison of water quality sensor deployment designs in wadeable streams. *Limnology and Oceanography: Methods*, 19(10), 673–681. <https://doi.org/10.1002/lom3.10452>
- Hensley, R. T., Kirk, L., Spangler, M., Gooseff, M. N., & Cohen, M. J. (2019). Flow extremes as spatiotemporal control points on river solute fluxes and metabolism. *Journal of Geophysical Research: Biogeosciences*, 124(3), 537–555. <https://doi.org/10.1029/2018JG004738>
- Hensley, R. T., McLaughlin, D. L., Cohen, M. J., & Decker, P. H. (2017). Stream phosphorus dynamics of minimally impacted coastal plain watersheds. *Hydrological Processes*, 31(8), 1636–1649. <https://doi.org/10.1002/hyp.11132>
- Hood, E., Gooseff, M. N., & Johnson, S. L. (2006). Changes in the character of stream water dissolved organic carbon during flushing in three small watersheds, Oregon. *Journal of Geophysical Research - Biogeosciences*, 111, G01007. <https://doi.org/10.1029/2005JG000082>
- Hood, E., McKnight, D., & Williams, M. W. (2003). Sources and chemical character of dissolved organic carbon (DOC) across an alpine/subalpine ecotone, Green Lakes valley, Colorado front range, USA. *Water Resources Research*, 39(7), 1188. <https://doi.org/10.1029/2002WR001738>
- Hood, E., Williams, M. W., & Caine, N. (2003). Landscape controls on organic and inorganic nitrogen leaching across an alpine-subalpine ecotone, Green Lakes valley, Colorado front range. *Ecosystems*, 6, 31–45. <https://doi.org/10.1007/s10021-002-0175-8>
- Hornberger, G. M., Bencala, K. E., & McKnight, D. M. (1994). Hydrological controls on dissolved organic carbon during snowmelt in the Snake River near Montezuma, Colorado. *Biogeochemistry*, 25(3), 147–165. <https://doi.org/10.1007/BF00024390>
- House, W. A., & Warwick, M. S. (1998). Hysteresis of the solute concentration/discharge relationship in rivers during storms. *Water Research*, 32(8), 2279–2290. [https://doi.org/10.1016/S0043-1354\(97\)00473-9](https://doi.org/10.1016/S0043-1354(97)00473-9)
- Jennings, K. S., & Molotch, N. P. (2020). Snowfall fraction, cold content, and energy balance changes drive differential response to simulated warming in an alpine and subalpine snowpack. *Frontiers in Earth Science*, 8, 186. <https://doi.org/10.3389/feart.2020.00186>
- Kampf, S. K., & Lefsky, M. A. (2016). Transition of dominant peak flow source from snowmelt to rainfall along the Colorado front range: Historical patterns, trends, and lessons from the 2013 Colorado Front Range floods. *Water Resources Research*, 52(1), 407–422. <https://doi.org/10.1002/2015WR017784>
- Kiewiet, L., van Meerveld, I., Stähli, M., & Seibert, J. (2020). Do stream water solute concentrations reflect when connectivity occurs in a small, pre-alpine headwater catchment? *Hydrology and Earth System Sciences*, 24(7), 3381–3398. <https://doi.org/10.5194/hess-24-3381-2020>
- Kirchner, J. W., Feng, X., & Neal, C. (2000). Fractal stream chemistry and its implications for contaminant transport in catchments. *Nature*, 403(6769), 524–527. <https://doi.org/10.1038/35000537>
- Kirchner, J. W., Feng, X. H., Neal, C., & Robson, A. J. (2004). The fine structure of water-quality dynamics: The (high-frequency) wave of the future. *Hydrological Processes*, 18(7), 1353–1359. <https://doi.org/10.1002/hyp.5537>
- Kirchner, J. W., Godsey, S. E., Osterhuber, R., McConnell, J. R., & Penna, D. (2020). The pulse of a montane ecosystem: Coupled daily cycles in solar flux, snowmelt, transpiration, groundwater, and streamflow at Sagehen and Independence creeks, Sierra Nevada, USA. *Hydrology and Earth System Sciences Discussions*, 2020, 1–46. <https://doi.org/10.5194/hess-2020-77>
- Knapp, J. L. A., von Freyberg, J., Studer, B., Kiewiet, L., & Kirchner, J. W. (2020). Concentration–discharge relationships vary among hydrological events, reflecting differences in event characteristics. *Hydrology and Earth System Sciences*, 24(5), 2561–2576. <https://doi.org/10.5194/hess-24-2561-2020>
- Koenig, L. E., Shattuck, M. D., Snyder, L. E., Potter, J. D., & McDowell, W. H. (2017). Deconstructing the effects of flow on DOC,

- nitrate, and major ion interactions using a high-frequency aquatic sensor network. *Water Resources Research*, 53(12), 10655–10673. <https://doi.org/10.1002/2017wr020739>
- Krogh, S.A., Scaff, L., Sterle, G., Kirchner, J., Gordon, B. and Harpold, A. (2021). Diel streamflow cycles suggest more sensitive snowmelt-driven streamflow to climate change than land surface modeling. *Hydrology and Earth System Sciences Discussions*. <https://doi.org/10.5194/hess-2021-437>
- Kurz, M. J., de Montety, V., Martin, J. B., Cohen, M. J., & Foster, C. R. (2013). Controls on diel metal cycles in a biologically productive carbonate-dominated river. *Chemical Geology*, 358, 61–74. <https://doi.org/10.1016/j.chemgeo.2013.08.042>
- Li, D., Wrzesien, M. L., Durand, M., Adam, J., & Lettenmaier, D. P. (2017). How much runoff originates as snow in the western United States, and how will that change in the future? *Geophysical Research Letters*, 44(12), 6163–6172. <https://doi.org/10.1002/2017GL073551>
- Litt, G. F., Gardner, C. B., Ogden, F. L., & Lyons, W. B. (2015). Hydrologic tracers and thresholds: A comparison of geochemical techniques for event-based stream hydrograph separation and flowpath interpretation across multiple land covers in the Panama Canal watershed. *Applied Geochemistry*, 63, 507–518. <https://doi.org/10.1016/j.apgeochem.2015.04.003>
- Lloyd, C. E. M., Freer, J. E., Johnes, P. J., & Collins, A. L. (2016). Using hysteresis analysis of high-resolution water quality monitoring data, including uncertainty, to infer controls on nutrient and sediment transfer in catchments. *The Science of the Total Environment*, 543, 388–404. <https://doi.org/10.1016/j.scitotenv.2015.11.028>
- Lunch, C.K., Laney, C.M. and NEON (National Ecological Observatory Network). (2021). neonUtilities: Utilities for Working with NEON data. R package version 2.1.3. <https://github.com/NEONScience/NEON-utilities>.
- Lundquist, J. D., & Cayan, D. R. (2002). Seasonal and spatial patterns in diurnal cycles in streamflow in the western United States. *Journal of Hydrometeorology*, 3(5), 591–603. [https://doi.org/10.1175/1525-7541\(2002\)003<0591:SASPID>2.0.CO;2](https://doi.org/10.1175/1525-7541(2002)003<0591:SASPID>2.0.CO;2)
- Marinos, R. E., Van Meter, K. J., & Basu, N. B. (2020). Is the river a Chemo-stat?: Scale versus land use controls on nitrate concentration-discharge dynamics in the upper Mississippi River basin. *Geophysical Research Letters*, 47(16), e2020GL087051. <https://doi.org/10.1029/2020GL087051>
- Marshall, A. M., Abatzoglou, J. T., Link, T. E., & Tennant, C. J. (2019). Projected changes in interannual variability of peak snowpack amount and timing in the Western United States. *Geophysical Research Letters*, 46(15), 8882–8892. <https://doi.org/10.1029/2019GL083770>
- McKnight, D. M., & Bencala, K. E. (1990). The chemistry of iron, aluminum, and dissolved organic material in three acidic, metal-enriched, mountain streams, as controlled by watershed and in-stream processes. *Water Resources Research*, 26(12), 3087–3100. <https://doi.org/10.1029/WR026i012p03087>
- Minaudo, C., Dupas, R., Gascuel-Oudou, C., Roubeyx, V., Danise, P. A., & Moatar, F. (2019). Seasonal and event-based concentration-discharge relationships to identify catchment controls on nutrient export regimes. *Advances in Water Resources*, 131, 103379. <https://doi.org/10.1016/j.advwatres.2019.103379>
- Mladenov, N., Williams, M. W., Schmidt, S. K., & Cawley, K. (2012). Atmospheric deposition as a source of carbon and nutrients to an alpine catchment of the Colorado Rocky Mountains. *Biogeosciences*, 9(8), 3337–3355. <https://doi.org/10.5194/bg-9-3337-2012>
- Moatar, F., Abbott, B. W., Minaudo, C., Curie, F., & Pinay, G. (2017). Elemental properties, hydrology, and biology interact to shape concentration-discharge curves for carbon, nutrients, sediment, and major ions. *Water Resources Research*, 53(2), 1270–1287. <https://doi.org/10.1002/2016WR019635>
- Mulholland, P. J., & Hill, W. R. (1997). Seasonal patterns in streamwater nutrient and dissolved organic carbon concentrations: Separating catchment flow path and in-stream effects. *Water Resources Research*, 33(6), 1297–1306. <https://doi.org/10.1029/97WR00490>
- Musolff, A., Fleckenstein, J. H., Rao, P. S. C., & Jawitz, J. W. (2017). Emergent archetype patterns of coupled hydrologic and biogeochemical responses in catchments. *Geophysical Research Letters*, 44(9), 4143–4151. <https://doi.org/10.1002/2017GL072630>
- Musolff, A., Zhan, Q., Dupas, R., Minaudo, C., Fleckenstein, J. H., Rode, M., Dehaspe, J., & Rinke, K. (2021). Spatial and temporal variability in concentration-discharge relationships at the event scale. *Water Resources Research*, 57(10), WR029442. <https://doi.org/10.1029/2020WR029442>
- NEON (National Ecological Observatory Network) 2021a. Continuous discharge (DP4.20130.001). <https://data.neonscience.org>.
- NEON (National Ecological Observatory Network) 2021b. Water quality (DP1.20288.001). <https://doi.org/10.48443/d8kw-5j62>.
- NEON (National Ecological Observatory Network) 2021c. Nitrate in surface water (DP1.20033.001). <https://doi.org/10.48443/924t-1k41>.
- NEON (National Ecological Observatory Network) 2021d. Chemical properties of surface water (DP1.20093.001). <https://doi.org/10.48443/05k7-e011>.
- Nimick, D. A., Gammons, C. H., & Parker, S. R. (2011). Diel biogeochemical processes and their effect on the aqueous chemistry of streams: A review. *Chemical Geology*, 283(1–2), 3–17. <https://doi.org/10.1016/j.chemgeo.2010.08.017>
- Oldani, K. M., Mladenov, N., Williams, M. W., Campbell, C. M., & Lipson, D. A. (2017). Seasonal patterns of dry deposition at a high-elevation site in the Colorado Rocky Mountains. *Journal of Geophysical Research: Atmospheres*, 122(20), 11–183. <https://doi.org/10.1002/2016JD026416>
- Oviedo-Vargas, D., Peipoch, M., & Dow, C. (2022). Metabolism and soil water viscosity control diel patterns of nitrate and DOC in a low order temperate stream. *Journal of Reophysical Research: Biogeosciences*, 127. <https://doi.org/10.1029/2021JG006640>
- Pellerin, B. A., Saraceno, J. F., Shanley, J. B., Sebestyen, S. D., Aiken, G. R., Wollheim, W. M., & Bergamaschi, B. A. (2012). Taking the pulse of snowmelt: In situ sensors reveal seasonal, event and diurnal patterns of nitrate and dissolved organic matter variability in an upland forest stream. *Biogeochemistry*, 108(1), 183–198. <https://doi.org/10.1007/s10533-011-9589-8>
- Pellerin, B. A., Stauffer, B. A., Young, D. A., Sullivan, D. J., Bricker, S. B., Walbridge, M. R., Clyde, G. A., Jr., & Shaw, D. M. (2016). Emerging tools for continuous nutrient monitoring networks: Sensors advancing science and water resources protection. *JAWRA Journal of the American Water Resources Association*, 52(4), 993–1008. <https://doi.org/10.1111/1752-1688.12386>
- Raymond, P. A., Saiers, J. E., & Sobczak, W. V. (2016). Hydrological and biogeochemical controls on watershed dissolved organic matter transport: Pulse-shunt concept. *Ecology*, 97(1), 5–16. <https://doi.org/10.1890/14-1684.1>
- Roberts, B. J., & Mulholland, P. J. (2007). In-stream biotic control on nutrient biogeochemistry in a forested stream, west fork of Walker branch. *Journal of geophysical research*. *Biogeosciences*, 112(G4). <https://doi.org/10.1029/2007JG000422>
- Rode, M., Angelstein, S. H. N., Anis, M. R., Borchardt, D., & Weitere, M. (2016). Continuous in-stream assimilatory nitrate uptake from high-frequency sensor measurements. *Environmental Science & Technology*, 50(11), 5685–5694. <https://doi.org/10.1021/acs.est.6b00943>
- Rode, M., Wade, A. J., Cohen, M. J., Hensley, R. T., Bowes, M. J., Kirchner, J. W., Arhonditsis, G. B., Jordan, P., Kronvang, B., Halliday, S. J., Skeffington, R. A., Rozemeijer, J. C., Aubert, A. H., Rinke, K., & Jomaa, S. (2016). Sensors in the stream: The high-frequency wave of the present. *Environmental Science & Technology*, 50(19), 10297–10307. <https://doi.org/10.1021/acs.est.6b02155>
- Rose, L. A., Karwan, D. L., & Godsey, S. E. (2018). Concentration–discharge relationships describe solute and sediment mobilization, reaction, and

- transport at event and longer timescales. *Hydrological Processes*, 32(18), 2829–2844. <https://doi.org/10.1002/hyp.13235>
- Rusjan, S., & Mikoš, M. (2010). Seasonal variability of diurnal in-stream nitrate concentration oscillations under hydrologically stable conditions. *Biogeochemistry*, 97(2–3), 123–140. <https://doi.org/10.1007/s10533-009-9361-5>
- Saraceno, J. F., Pellerin, B. A., Downing, B. D., Boss, E., Bachard, P. A., & Bergamaschi, B. A. (2009). High-frequency in situ optical measurements during a storm event: Assessing relationships between dissolved organic matter, sediment concentrations, and hydrological processes. *Journal of Geophysical Research: Biogeosciences*, 114(G4). <https://doi.org/10.1029/2009JG000989>
- Savoy, P., & Harvey, J. W. (2021). Predicting light regime controls on primary productivity across CONUS river networks. *Geophysical Research Letters*, 48(10), GL092149. <https://doi.org/10.1029/2020GL092149>
- Sueker, J. K., Clow, D. W., Ryan, J. N., & Jarrett, R. D. (2001). Effect of basin physical characteristics on solute fluxes in nine alpine/subalpine basins, Colorado, USA. *Hydrological Processes*, 15(14), 2749–2769. <https://doi.org/10.1002/hyp.265>
- Sullivan, A. B., Drever, J. I., & McKnight, D. M. (1998). Diel variation in element concentrations, Peru Creek, Summit County, Colorado. *Journal of Geochemical Exploration*, 64(1–3), 141–145. [https://doi.org/10.1016/S0375-6742\(98\)00027-2](https://doi.org/10.1016/S0375-6742(98)00027-2)
- Thompson, S. E., Basu, N. B., Lascrain, J., Aubeneau, A., & Rao, P. S. C. (2011). Relative dominance of hydrologic versus biogeochemical factors on solute export across impact gradients. *Water Resources Research*, 47 (W00J05). <https://doi.org/10.1029/2010wr009605>
- Thompson, S. E., & Katul, G. G. (2012). Multiple mechanisms generate Lorentzian and  $1/f$   $\alpha$  power spectra in daily stream-flow time series. *Advances in Water Resources*, 37, 94–103. <https://doi.org/10.1016/j.advwatres.2011.10.010>
- Vaughan, M. C. H., Bowden, W. B., Shanley, J. B., Vermilyea, A., Sleeper, R., Gold, A. J., Pradhanang, S. M., Inamdar, S. P., Levia, D. F., Andres, A. S., Birgand, F., & Schroth, A. W. (2017). High-frequency dissolved organic carbon and nitrate measurements reveal differences in storm hysteresis and loading in relation to land cover and seasonality. *Water Resources Research*, 53(7), 5345–5363. <https://doi.org/10.1002/2017wr020491>
- von Freyberg, J., Studer, B., & Kirchner, J. W. (2017). A lab in the field: High-frequency analysis of water quality and stable isotopes in stream water and precipitation. *Hydrology and Earth System Sciences*, 21(3), 1721–1739. <https://doi.org/10.5194/hess-21-1721-2017>
- Werner, B. J., Musolff, A., Lechtenfeld, O. J., de Rooij, G. H., Oosterwoud, M. R., & Fleckenstein, J. H. (2019). High-frequency measurements explain quantity and quality of dissolved organic carbon mobilization in a headwater catchment. *Biogeosciences*, 16(22), 4497–4516. <https://doi.org/10.5194/bg-16-4497-2019>
- Williams, M. (2021). Stream water chemistry data for Como creek, 1998–2013 ver 1. *Environmental Data Initiative*. <https://doi.org/10.6073/pasta/203daf080eae3403e1f900292c4fd0fb>
- Williams, M., Knowles, J., Cowie, R., & Niwot Ridge, L. T. E. R. (2021). Stream-flow data for Como creek, 2006–2014 ver 1. *Environmental Data Initiative*. <https://doi.org/10.6073/pasta/82fd3feabda2b0e200ef4b85bc18a5ea>
- Williams, M. K., Seibold, C., & Chowanski, K. (2009). Storage and release of solutes from a subalpine seasonal snowpack: Soil and stream water response, Niwot Ridge, Colorado. *Biogeochemistry*, 95, 77–94. <https://doi.org/10.1007/s10533-009-9288-x>
- Williams, M. W., Baron, J., Caine, N., Sommerfeld, R., & Sanford, R. (1996). Nitrogen saturation in the Colorado front range. *Environmental Science and Technology*, 30, 640–646. <https://doi.org/10.1021/es950383e>
- Williams, M. W., & Melack, J. M. (1991). Solute chemistry of snowmelt and runoff in an alpine basin, Sierra Nevada. *Water Resources Research*, 27(7), 1575–1588. <https://doi.org/10.1029/90WR02774>
- Wollheim, W. M., Mulukutla, G. K., Cook, C., & Carey, R. O. (2017). Aquatic nitrate retention at river network scales across flow conditions determined using nested in situ sensors. *Water Resources Research*, 53(11), 9740–9756. <https://doi.org/10.1002/2017wr020644>
- Zeileis, A., Grothendieck, G., Ryan, J.A., Ulrich, J.M., and Andrews, F. (2022). Zoo: S3 infrastructure for regular and irregular time series. R package version 1.8–10. <https://CRAN.R-project.org/package=zoo>.

## SUPPORTING INFORMATION

Additional supporting information can be found online in the Supporting Information section at the end of this article.

**How to cite this article:** Hensley, R., Singley, J., & Gooseff, M. (2022). Pulses within pulses: Concentration-discharge relationships across temporal scales in a snowmelt-dominated Rocky Mountain catchment. *Hydrological Processes*, 36(9), e14700. <https://doi.org/10.1002/hyp.14700>